21st Australasian Fluid Mechanics Conference
Adelaide, Australia
10-13 December 2018

Nucleation Effects on Hydrofoil Tip Vortex Cavitation

M. T. Khoo[1,2], J. A. Venning[2], B. W. Pearce[2] and P. A. Brandner[2]

[1]Maritime Division
Defence Science and Technology Group, Fishermans Bend, Victoria, 3207, Australia

[2]Australian Maritime College
University of Tasmania, Launceston, Tasmania, 7250, Australia

Abstract

Tip vortex cavitation inception about an elliptical planform, NACA 0012 hydrofoil is investigated in cavitation tunnel flows in which cavitation nuclei are deplete and abundant. Tests were conducted at fixed Reynolds and cavitation numbers. The onset, or inception, of cavitation was induced by increasing the angle of incidence and behaviour was recorded photographically and acoustically. Cavitation inception occurred at a higher incidence in the deplete case compared with the abundant due to fewer weaker nuclei. It also occurred within a small incidence change for the deplete case, with the appearance of a continuous, cavitating vortical flow structure. Whereas for the abundant case, inception was intermittent, occurring across a larger incidence range. This was associated with individual nuclei activation events increasing in frequency with increasing incidence. Sound pressure levels increased with inception and cavity development but reduced to a local minimum once the cavity attached to the hydrofoil, increasing thereafter with incidence. Overall sound levels were higher for the abundant case than for the deplete case.

Introduction

Cavitation occurs when a fluid changes from liquid to vapour phase due to pressure reduction. Tip Vortex Cavitation (TVC) is often the first form of cavitation to occur due to the low pressure generated in the vortex core [3, 7]. A tip vortex is generated at the tip of a lifting surface operating at non-zero lift.

Microbubbles, and potentially gas-containing biological organisms or solid particles with trapped gas [12], provide nuclei for cavitation inception. Nuclei are captured in vortical flows due to buoyancy created by the radial pressure gradient. A captured microbubble will trigger inception if the core pressure is below a size-dependent critical pressure less than vapour pressure. Microbubble equilibrium then becomes unstable—it will grow explosively and fill with vapour leading to macroscopic cavitation formation. TVC inception and development generates noise due to complex transients [5] and modes of oscillation [14].

Typically, practical flows contain a range of nuclei sizes at differing concentrations making TVC inception a complex probabilistic process. The nuclei deplete and abundant flows that are possible in the AMC cavitation tunnel allow the effects of nuclei content on TVC inception to be quantified, the results of which have implications for ship and submarine operations.

The definition of TVC inception is not entirely clear. The challenge of visually detecting inception is related to the difficulty of distinguishing a vaporous cavity from migration of nuclei into the vortex core with high nuclei concentration flows [1]. Two definitions of inception have been proposed: 1) the first appearance of a cavitation bubble and 2) the persistent attachment of a vapour core to the foil tip. Similar definitions were used for visual detection in [10], with the exception that a coalesced, persistent cavity within 0.2 chord lengths downstream of the hydrofoil tip was also considered to be 'attached'.

Criteria for TVC inception using acoustic measurements have also been proposed. An event rate threshold of one per second was used as an inception criterion in [4], the results of which correlated well with those for visual detection using the same event rate threshold. In a separate study, a detection threshold of 3 dB above the background level was used for propeller cavitation inception [8]. Using this approach, inception numbers from acoustic measurements were approximately 5–10% higher than for visual detection, regardless of nuclei population.

TVC behaviour at inception has also been documented in several studies [1]. Using visual observations and increasing the angle of incidence, the first appearance of a cavitation bubble occurred at lower incidence in a flow seeded with microbubbles compared with an unseeded flow. In contrast, permanent attachment of the vapour core to the foil tip occurred at practically the same incidence regardless of seeding conditions.

The sound level of propeller cavitation during cavity development was observed to increase monotonically with decreasing cavitation number [8]. In contrast, a local peak was observed when cavitation desinence of a hydrofoil was studied by increasing the cavitation number [16]. It was also found that the maximum sound level increased with nuclei concentration.

A literature review reveals little published data on nucleation effects on hydrofoil TVC inception using correlated acoustic and visual measurements. To gain further insight into the effects of nuclei on TVC inception, flow physics and sound levels, experiments were carried out at the Australian Maritime College Cavitation Research Laboratory (AMC CRL) using an elliptical planform, NACA 0012 hydrofoil to address this gap. Only a limited number of cavitation test facilities currently exist which allow strict control over nuclei content in the water [2, 13, 16]. Two extreme cases of flows with a low concentration of small nuclei (referred to as 'deplete') and a high concentration of large nuclei ('abundant') were considered, with TVC inception behaviour measured both photographically and acoustically.

Experimental overview

TVC inception measurements were carried out in the cavitation tunnel at the AMC CRL. The test section is 0.6×0.6 m in cross section and 2.6 m long. The circuit volume is 365 m^3 and demineralised water is used as the working fluid. The absolute pressure at the centreline of the test section can be set between 4–400 kPa and the flow velocity can be varied between 2–12 m/s. The tunnel has ancilliaries for fast degassing and nuclei injection, and flow conditioning for continuous elimination of microbubbles enabling strict control of nuclei content. Further details on tunnel design and operation are described in [2].

The model hydrofoil is of elliptical planform, NACA 0012 section profile, 150 mm base chord and aspect ratio of 1.5 (defined as $\mathcal{AR} = b^2/A$, where b is the span and A is the planform area).

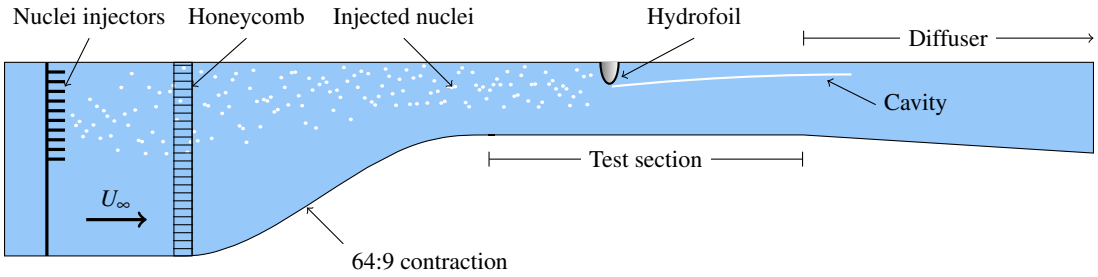

Figure 1: Schematic of the hydrofoil TVC experimental setup. Hydrophone and cameras are not shown. For the seeded case, microbubbles are injected from upstream of the test section through an array of injectors.

It was ceiling-mounted nominally midway along the tunnel test section, as shown in figure 1. All experiments were conducted at a fixed Reynolds number, Re, of 2×10^6 (using base chord as the characteristic length) and cavitation number, σ of 1.0, where $Re = U_\infty c/\nu$ and $\sigma = (p_\infty - p_v)/q$, where U_∞ is the freestream velocity, c the base chord, ν the kinematic viscosity, p_∞ the freestream pressure, p_v the vapour pressure and q the dynamic pressure. The model incidence was set using an automated force balance via closed loop control.

Cumulative histograms of nuclei concentration as a function of critical pressure relative to vapour pressure ($T_c = p_c - p_v$), for the nuclei deplete and abundant cases are shown in figure 2. The nuclei deplete case is the naturally occurring background population in the tunnel which is not active for many forms of cavitation [17] but may be so for TVC given the high tensions developed in vortex cores. This background population is too sparse and small for practical measurement with optical techniques and have been measured with a Cavitation Susceptibility Meter (CSM) [11]. Water is sampled from the tunnel resorber and passed through a venturi at different throat pressures, resulting in a cumulative histogram of concentration against T_c. The abundant nuclei case is created using a 3×10 rectangular array of microbubble generators each directly injecting about 10^6 bubbles per second. The array is located upstream of the contraction, as shown in figure 1. This population was measured in the test section upstream of the hydrofoil using Interferometric Mie Imaging (IMI) [15]. The CSM measurement produces a cumulative histogram whereas the IMI provides a histogram of concentration per unit size increment. These can be compared through numerical integration of the cumulative histogram:

$$C(T_c) = \int_{T_{c_{max}}}^{T_c} c(T_c)\, dT_c \qquad (1)$$

where C is the concentration of all nuclei with critical pressures greater than T_c and c is the concentration density. The initial bubble diameter, D_∞, corresponding to T_c can be found numerically from single bubble equilibrium theory [7]:

$$\frac{4}{27{T_c}^2} = \left(\frac{D_\infty}{4S}\right)^3 (p_\infty - p_v) + \left(\frac{D_\infty}{4S}\right)^2 \qquad (2)$$

where S is the surface tension.

Two approaches were used to detect TVC. Firstly, a digital single-lens reflex camera was used to take photographs near the hydrofoil tip at each test condition prior to and after inception. Acoustic measurements were taken for the corresponding test conditions using an in-ceiling hydrophone [6] (Brüel&Kjær Type 8103, sample rate 204.8 kHz) located $2.5c$ downstream of the hydrofoil. The Sound Pressure Level (SPL) was calculated from the integral of the power spectral density (Hanning window in 1 s blocks, shifted by 1/8 s with one-third octave bands) across the range of measured frequencies [9]. A lower cutoff

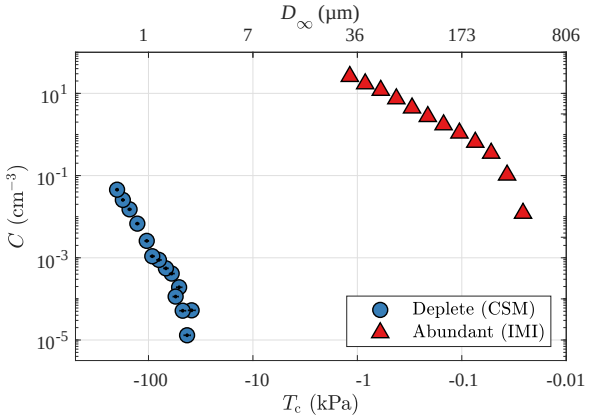

Figure 2: Deplete and abundant nuclei distributions measured using CSM and IMI methods respectively. For CSM measurements, water was sampled from the tunnel resorber. IMI measurements were taken in the test section.

frequency of 400 Hz was used to exclude frequencies not directly associated with the tip vortex cavity. The SPL in the nth band is calculated by

$$\mathrm{SPL}_n = 10\log_{10}\left(\frac{1}{p_{\mathrm{ref}}^2}\int_{f_l^{(n)}}^{f_u^{(n)}} G_{pp}(f)\, df\right) \mathrm{dB\,re}\, p_{\mathrm{ref}} \qquad (3)$$

where p_{ref} is the reference pressure (1 μPa), $f_l^{(n)}$ and $f_u^{(n)}$ are the lower and upper frequency of the nth band respectively, G_{pp} is the single-sided spectrum and f is the frequency.

The angle of incidence of the hydrofoil was increased while σ and Re were held constant. This enabled the injector settings to be maintained as constant. Starting from $\alpha = 0°$, preliminary runs were conducted by continuously increasing α to identify the approximate inception angles, α_i. Photographs and acoustic measurements were taken at $\alpha = 0°$, then α was increased with coarse resolution (0.5–1°). Finer resolution (0.1°) was used just prior to and just after α_i. The hydrofoil remained at each α for approximately 50 s, including 20 s of acoustic measurements.

Results

The changes in SPL with increasing α for the nuclei deplete and abundant cases are shown in figure 3. The red, dotted line represents a SPL of 3 dB above the background level measured at $\alpha = 0°$. TVC photographs are provided for α values corresponding to salient features on the SPL graph.

For the deplete case, inception occurs at $\alpha = 5.9°$ with the appearance of a continuous tip vortex cavity, the leading edge of which is just downstream of the hydrofoil tip. With inception, the SPL rises by about 5 dB. The cavity has a bulbous leading edge with a necked region immediately downstream suggesting the presence of re-entrant flow. Perturbations or waves can

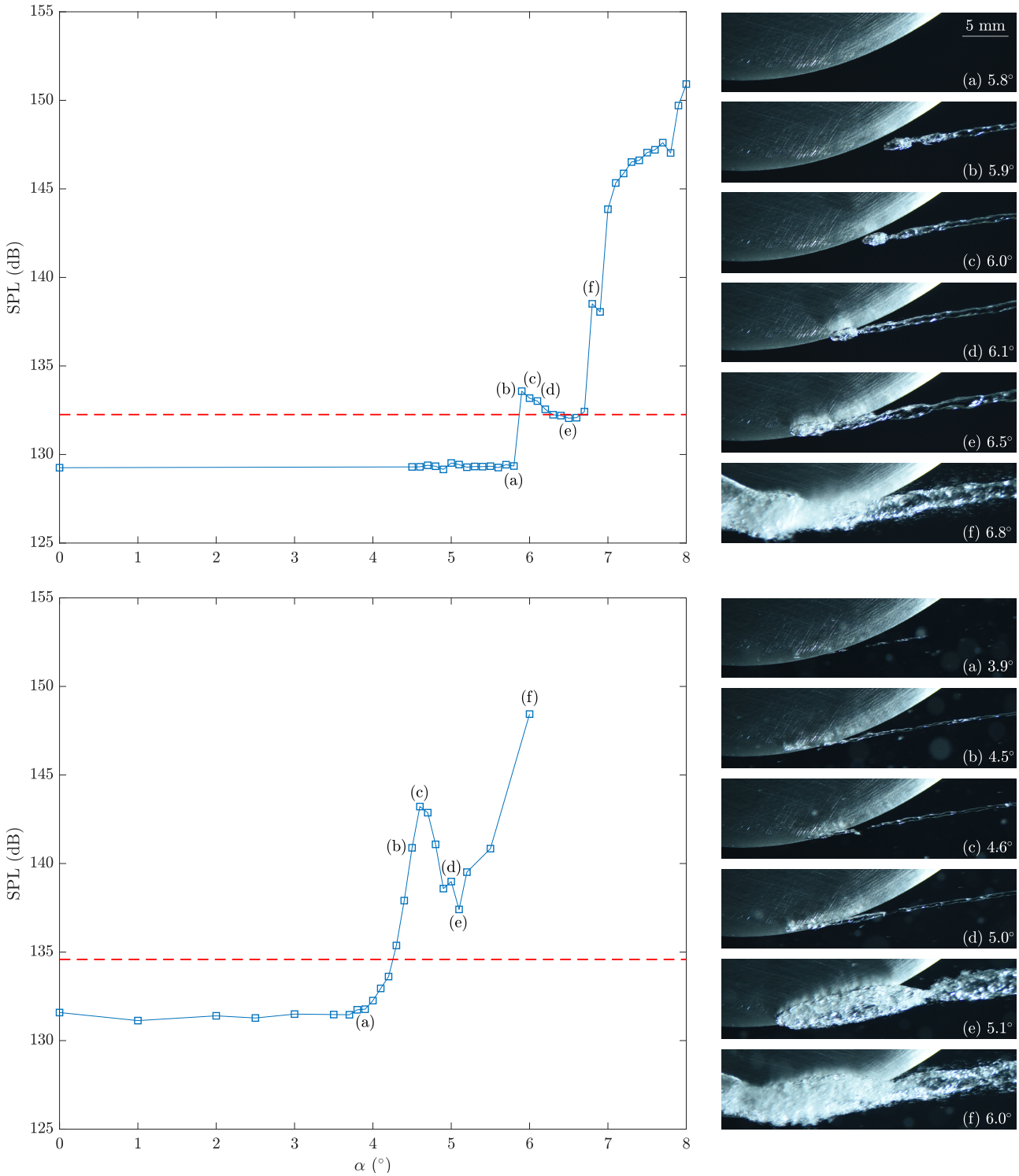

Figure 3: Change of Sound Pressure Level, SPL, with angle of incidence, α, without (top) and with (bottom) seeding for $\sigma = 1.0$ and $Re = 2 \times 10^6$. Red, dotted lines represent thresholds 3 dB above the background levels measured at $\alpha = 0°$. Photographs of the cavity are provided for angles of interest.

be seen on the cavity due to various cavity deformation modes [14]. The TVC moves upstream with increasing α accompanied by a decrease in SPL. The TVC reaches the hydrofoil outline by 6.1° and moves within the outline by 6.5°. At this α the leading edge flow appears suppressed which may be associated with the drop in SPL. The SPL increases again with α, with a large increase occurring at 6.8° associated with TVC attachment and the formation of hydrofoil leading edge sheet cavitation. The SPL increases further with α due to sheet cavitation growth.

For the abundant case the pre-inception SPL is about 2 dB greater than the nuclei deplete case. This may be attributable to nuclei injector operation upstream, but perhaps more likely, excitation or deformation of nuclei in the flow. Inception in this case does not occur with a 0.1° change in α, as with the deplete case, but is a process that starts with intermittent nuclei capture and activation events which progress with increasing event rate to a sustained continuous cavity. This process starts at a much smaller α than for the deplete case due to the greater concentration of larger, weaker nuclei. Intermittent capture events are visible at about 2° but the SPL only begins to rise at about 3.9°. The cavity remains discontinuous with increasing α to 4.5° where it extends upstream to within the hydrofoil planform, and to 4.6° where the SPL reaches a local maximum. The extent of the intermittency decreases with increasing α and the cavity becomes continuous downstream of the hydrofoil planform at about $\alpha = 5.0^\circ$ but is unsteady upstream of this point.

The increase in SPL with α up to 4.6° is presumably due to the increasing nuclei capture/activation rate and the local maximum is due to this rate also reaching a maximum. That is, for higher α this rate reduces with greater sustained cavity length, hence the reduction in SPL. The SPL reaches a local minimum at $\alpha = 5.1^\circ$ where the cavity increases in diameter and becomes attached to the hydrofoil. For further α increase, the SPL increases with the formation of sheet cavitation as occurred for the nuclei deplete case.

The local SPL maximum that occurs after inception with TVC development is much higher for the abundant case than for the deplete case showing that intermittent nuclei activations generate higher SPL than local flow features or continuous cavity modes. The cavity diameter during initial development is much less than for the deplete case which may be attributable to reduced boundary layer thickness at lower α or more significantly intermittency reducing the volume of dissolved gas diffusing from the liquid to the cavity. This is driven by the concentration gradient between the vapour/gaseous cavity and the liquid. This is evidenced by the similar cavity diameters and volumes that form once the cavity becomes persistent.

Conclusion

Tip vortex cavitation inception has been investigated about an elliptical hydrofoil in nuclei deplete and abundant flows using photographic and acoustic measurements. For the deplete case, inception occurred within a 0.1° angle of incidence change resulting in the sudden appearance of a continuous cavity and step change in sound pressure level. For the abundant case, inception occurred at lower incidence due to a higher concentration of weaker nuclei. For this case, inception involved intermittency associated with individual activation events increasing in frequency with incidence until a continuous cavity was sustained. This process occurred over a range of incidences and was accompanied by increasing sound levels to a local maximum possibly associated with a maximum cavitation rate.

Both cases exhibit local maxima in sound pressure level associated with inception or development although each appears associated with different cavity physics. Overall sound levels are much higher in the abundant case. These levels reached local minima with cavity hydrofoil attachment before increasing with incidence due to sheet cavity formation.

Acknowledgements

The authors acknowledge the support of the University of Tasmania and AMC technical officers Mr Robert Wrigley and Mr Steven Kent.

References

[1] Boulon, O., Franc, J.-P. and Michel, J.-M., Tip vortex cavitation on an oscillating hydrofoil, *J. Fluids Eng.*, **119**, 1997, 752–758.

[2] Brandner, P., Lecoffre, Y. and Walker, G., Design considerations in the development of a modern cavitation tunnel, in *16th Australasian Fluid Mechanics Conf.*, 2007.

[3] Brennen, C. E., *Cavitation and Bubble Dynamics*, Cambridge University Press, 1995.

[4] Briançon-Marjollet, L. and Merle, L., Inception, development and noise of a tip vortex cavitation, in *Proc. 21st Symp. Naval Hydrodynamics*, 1996, 851–864.

[5] Choi, J. and Ceccio, S. L., Dynamics and noise emission of vortex cavitation bubbles, *J. Fluid Mech.*, **575**, 2007, 1–26.

[6] Doolan, C., Brandner, P., Butler, D., Pearce, B., Moreau, D. and Brooks, L., Hydroacoustic characterisation of the AMC cavitation tunnel, in *Acoustics 2013 Victor Harbor: Science, Technology and Amenity*, 2013, 1–7.

[7] Franc, J.-P. and Michel, J.-M., *Fundamentals of Cavitation*, Springer Science & Business Media, 2006.

[8] Gindroz, B. and Billet, M., Nuclei and propeller cavitation inception, Technical report, American Society of Mechanical Engineers, NY (United States), 1994.

[9] Glegg, S. and Devenport, W., *Aeroacoustics of Low Mach Number Flows: Fundamentals, Analysis, and Measurement*, Academic Press, 2017.

[10] Gowing, S., Briançon-Marjollet, L., Frechou, D. and Godeffroy, V., Dissolved gas and nuclei effects on tip vortex cavitation inception and cavitating core size, in *Proc. 5th Int. Symp. Cavitation*, 1995, 173–180.

[11] Khoo, M., Venning, J., Pearce, B., Brandner, P. and Lecoffre, Y., Development of a cavitation susceptibility meter for nuclei size distribution measurements, in *20th Australasian Fluid Mechanics Conf.*, 2016.

[12] Lecoffre, Y., *Cavitation Bubble Trackers*, A. A. Balkema, 1999.

[13] Lecoffre, Y., Chantrel, P. and Teiller, J., Le grand tunnel hydrodynamique (GTH), *La Houille Blanche*, 585–592.

[14] Pennings, P., Bosschers, J., Westerweel, J. and Van Terwisga, T., Dynamics of isolated vortex cavitation, *J. Fluid Mech.*, **778**, 2015, 288–313.

[15] Russell, P. S., Venning, J. A., Brandner, P. A., Pearce, B. W., Giosio, D. R. and Ceccio, S. L., Microbubble disperse flow about a lifting surface, in *32nd Symp. Naval Hydrodynamics*, 2018.

[16] Song, M., Xu, L., Peng, X. and Tang, D., An acoustic approach to determine tip vortex cavitation inception for an elliptical hydrofoil considering nuclei-seeding, *Int. J. Multiph. Flow*, **90**, 2017, 79–87.

[17] Venning, J., Khoo, M., Pearce, B. and Brandner, P., Background nuclei measurements and implications for cavitation inception in hydrodynamic test facilities, *Exp. Fluids*, **59**, 2018, 71.